1P022

Ultrafast hydrogen migration in 1,3-butadiene in intense laser fields studied by coincidence momentum imaging

(Department of Chemistry, School of Science, The University of Tokyo)
◊H.L. Xu, T. Okino, K. Yamanouchi
(Photonics Institute, Vienna University of Technology, Vienna, Austria)
Stefan Roither, Xinhua Xie, Daniil Kartashov, Andrius Baltuska, and Markus Kitzler

[Introduction]

During the past few years, an ultrafast hydrogen migration process within a molecule in intense laser fields has been an attractive research theme, not only because of the findings that hydrogen atoms (or protons) move extremely rapidly within a molecule, but also their potential applicability for controlling chemical bond breaking processes [1]. The hydrogen migration process, in which hydrogen atom(s) or proton(s) migrate from one site to another within a molecule, can induce large scale deformation of molecular skeletal structure and rearrangement of chemical bonds. In the present study, two-body dissociation processes of doubly charged 1,3-butadiene ($H_2CCHCHCH_2^{2+}$) induced by intense laser fields are investigated by the coincidence momentum imaging (CMI) method. From the CMI maps, four dissociation pathways, $C_4H_6^{2+} \rightarrow C_2H_m^+ + C_2H_{6-m}^+$ (m =2, 3) and $C_4H_6^{2+}$ $CH_n^+ + C_3H_{6-n}^+$ (n =2, 3), are identified. The formation of CH_3^+ and $C_2H_4^+$ in the two-body dissociation processes clearly proves that the chemical bond rearrangement associated with an ultrafast hydrogen migration in the intense laser field occurs prior to the dissociation. It is found that the hydrogen atom bonded originally to one of the two central carbon positions tends to move to its neighboring methylene group to form a methyl group.

[Experiments]

The laser pulses (795 nm, ~40 fs, ~2.2×10^{14} W/cm^2), generated by a 5 kHz Ti: Sapphire laser system, were focused through a quartz lens (f =15 cm) onto a sample molecular beam of 1,3-butadiene in an ultrahigh vacuum chamber. The base pressure of the ultrahigh vacuum chamber is about ~3×10^{-11} Torr. In order to avoid false coincidence events originating from the fragment ions generated from two or more parent ions, the pressure in the main chamber was kept to be ~1.3×10^{-10} Torr, so that the number of events of the generation of ion species per laser shot was ~0.5 events/pulse. The laser polarization direction, electrode plates, and the surface of the detector were all set to be parallel to the plane formed by the laser and molecular beams. The three-dimensional momentum vectors of i-th fragment ions were determined by their position (x_i, y_i) and arrival time (t_i) on the detector plane [2].

[Results and Discussion]

In Fig. 1, the two-dimensional coincidence momentum maps of the fragment ions $C_2H_3^+$, CH_2^+, $C_2H_2^+$, and CH_3^+, recorded in coincidence with $C_2H_3^+$, $C_3H_4^+$, $C_2H_4^+$ and $C_3H_3^+$, respectively, are shown. Therefore, two types of the two-body Coulomb explosion pathways from the doubly charged parent ion, $C_4H_6^{2+}$ are securely identified, i.e., pathways in which one of the two terminal C-C bonds is broken, (1) $C_4H_6^{2+} \rightarrow CH_2^+ + C_3H_4^+$ and (2) $C_4H_6^{2+} \rightarrow CH_3^+ + C_3H_3^+$, and pathways in which the central C-C bond is broken, (3) $C_4H_6^{2+} \rightarrow C_2H_2^+ + C_2H_4^+$ and (4) $C_4H_6^{2+} \rightarrow C_2H_3^+ + C_2H_3^+$. It can be seen that in the dissociation pathways (1) and (4), a C-C chemical bond is broken without migration of a hydrogen atom within a parent molecule, while in the pathways (2) and (3), the fragment ions can only be generated though C-C bond breakings after at least a hydrogen atom migrates within a parent molecule.

From the CMI maps, ~4.1×10^5 and ~6.6×10^3 events are identified as coincidence events for the pathways (2) and (3), respectively. The relative yields of $C_2H_2^+$ in the pathway

(3) with respect to that of CH_3^+ in the pathway (2) is thus ~ 0.02. This may indicate that the precursor species, $CH_3^+ \cdots C_3H_3^+$, is much easier to be formed than the precursor species, $C_2H_2^+ \cdots C_2H_4^+$. Considering that if the hydrogen atom located at one of the two central carbon positions moves to its neighboring methylene group, the precursor species $CH_3^+ \cdots C_3H_3^+$ is formed, vice versa, the precursor species $C_2H_2^+ \cdots C_2H_4^+$ is formed, the much more ion yield of CH_3^+ than $C_2H_2^+$ suggests that in the intense laser field the hydrogen atom located at one of the two central carbon positions tends to move to its neighboring methylene group.

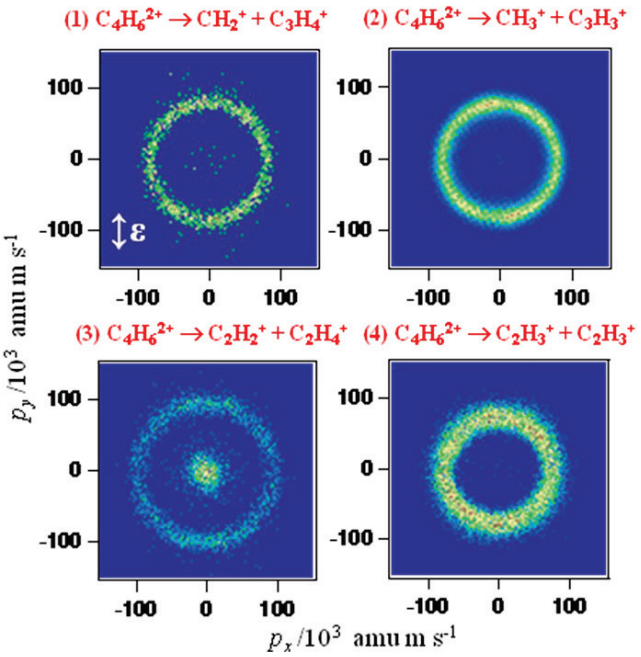

Fig. 1. Slices of the three-dimensional coincidence momentum sphere of the fragments resulting from intense laser induced two-body dissociation of $C_4H_6^{2+}$. The slices are presented in the p_x-p_y plane. The laser polarization direction (ε) was set to be parallel to the p_y axis as indicated by the arrow. The momentum distribution of only one of the two fragment ion species is shown because that of the other fragment ion species is related by the simple momentum conservation. The ranges of the momentum vector distribution along the z axis are : (i) $|p_z| < 50\times10^3$ amu m s^{-1} for CH_2^+, (ii) $|p_z| < 50\times10^3$ amu m s^{-1} for CH_3^+, (iii) $|p_z| < 50\times10^3$ amu m s^{-1} for $C_2H_2^+$, and (iv) $70\times10^3 < |p_z| < 80\times10^3$ amu m s^{-1} for $C_2H_3^+$.

It is remarkable that all four fragmentation pathways show almost isotropic distributions regardless of whether a hydrogen atom migrates during the dissociation or not, as can be seen from the CMI maps in Fig. 1. Therefore, the structural geometry changes (isomerization) of the precursor species induced by the hydrogen migration may play a negligible role in determining the four almost homogeneous distributions of the observed momentum maps. We assign here the four isotropic distributions to a combination of the bent skeletal structure of the parent molecule which results in the recoil direction of the fragment ions off the laser polarization direction, and the overall rotational motion of the molecule during the dissociation process.

Furthermore, from the three-dimensional momentum distributions of the fragment ions, the distributions of the released kinetic energy E_{kin} for the four explosion pathways are obtained. It was found that (i) the KER is higher for the bond breaking at the central bond (4.3 eV) than for the bond breaking at the terminal bond (3.4 eV), and (ii) the KER distribution is narrower for the bond breaking at the terminal bond (FWHM 0.7 eV) than for the bond breaking at the central bond (1.2 eV).

Reference

[1] H. Xu, T. Okino, and K. Yamanouchi, *Chem. Phys. Lett.* **469**, 255 (2009)
[2] H. Hasegawa, A. Hishikawa, and K. Yamanouchi, *Chem. Phys. Lett.* **349**, 57 (2001)